ADVANCED HEALTHCARE MATERIALS

Supporting Information

for *Adv. Healthcare Mater.*, DOI: 10.1002/adhm.201900612

Cell Membrane-Coated Magnetic Nanocubes with a Homotypic Targeting Ability Increase Intracellular Temperature due to ROS Scavenging and Act as a Versatile Theranostic System for Glioblastoma Multiforme

Christos Tapeinos, Francesca Tomatis, Matteo Battaglini, Aitor Larrañaga, Attilio Marino, Iker Aguirrezabal Telleria, Makis Angelakeris, Doriana Debellis, Filippo Drago, Francesca Brero, Paolo Arosio, Alessandro Lascialfari, Andrea Petretto, Edoardo Sinibaldi, and Gianni Ciofani**

Supporting information

Cell membrane-coated magnetic nanocubes with a homotypic targeting ability increase intracellular temperature due to ROS scavenging and act as a versatile theranostic system for glioblastoma multiforme

Christos Tapeinos[a,†,], Francesca Tomatis[b,†], Matteo Battaglini[a,c], Aitor Larrañaga[d], Attilio Marino[a], Iker Aguirrezabal Telleria[e], Angelakeris Makis[f], Doriana Debellis[g], Filippo Drago[h] Francesca Brero[i], Paolo Arosio[j], Alessandro Lascialfari[j], Andrea Petretto[k], Edoardo Sinibaldi[l], Gianni Ciofani [a,b,*]*

[a]Smart Bio-Interfaces, Istituto Italiano di Tecnologia, 56025 Pontedera, Italy

[b]Department of Mechanical and Aerospace Engineering, Politecnico di Torino, 10129 Torino, Italy

[c]The Biorobotics Institute, Scuola Superiore Sant'Anna, 56025 Pontedera, Italy

[d]Department of Mining-Metallurgy Engineering and Materials Science & POLYMAT, University of the Basque Country, 48013 Bilbao, Spain

[e]Department of Chemical and Environmental Engineering, Engineering School of the University of the Basque Country (UPV/EHU), 48013 Bilbao, Spain

[f] Department of Physics, Aristotle University of Thessaloniki, 54124 Thessaloniki, Greece

[g]Electron microscopy facility, Istituto Italiano di Tecnologia, 16163 Genova, Italy

[h]Nanochemistry Department, Istituto Italiano di Tecnologia, Genova, 16163 Italy

[i]Department of Physics and INSTM, Università degli Studi di Pavia, 27100 Pavia, Italy

[j]Department of Physics and INSTM, Università degli Studi di Milano, 20133 Milano, Italy

[k]Core Facilities-Clinical Proteomics and Metabolomics Laboratory, IRCCS Istituto Giannina Gaslini, 16147 Genova, Italy

[I]Center for Micro-BioRobotics, Istituto Italiano di Tecnologia, 56025 Pontedera, Italy

[†] These authors equally contributed to this work

[*] Corresponding authors: christos.tapeinos@iit.it, gianni.ciofani@iit.it

Transmission Electron microscopy

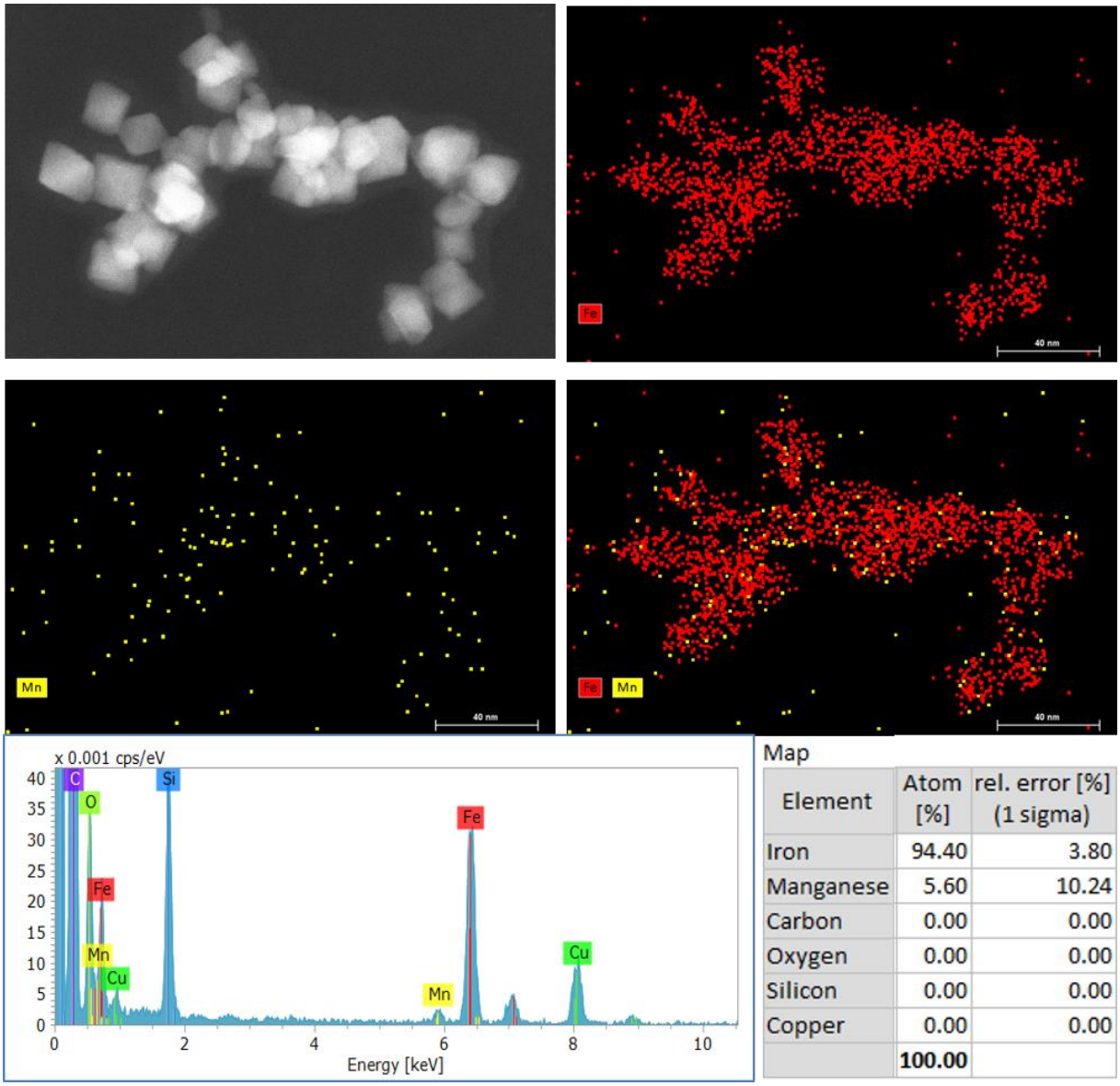

Map

Element	Atom [%]	rel. error [%] (1 sigma)
Iron	94.40	3.80
Manganese	5.60	10.24
Carbon	0.00	0.00
Oxygen	0.00	0.00
Silicon	0.00	0.00
Copper	0.00	0.00
	100.00	

Figure S1. Transmission electron micrograph and electron dispersive x-ray analysis of the plain NCubes

X-ray diffraction

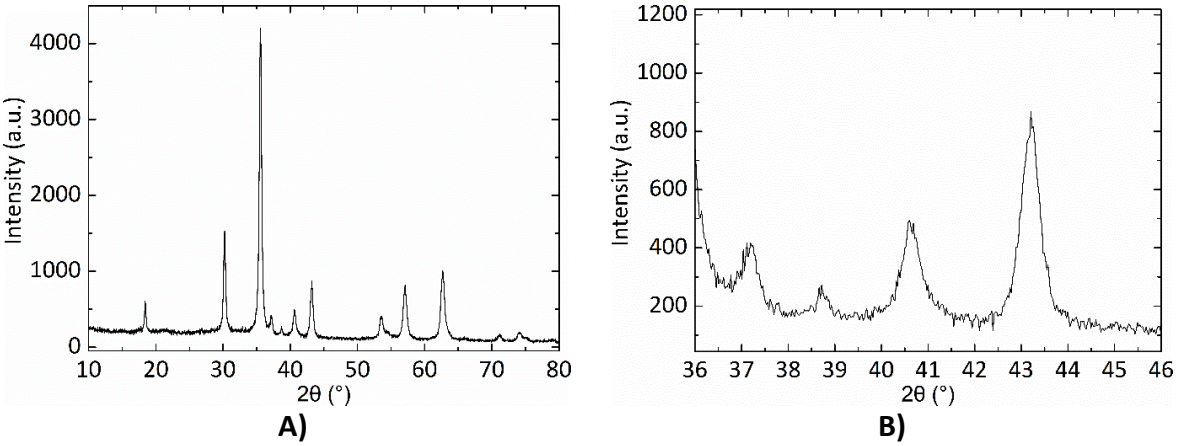

Figure S2. A) X-ray diffraction spectrum of CM-NCubes and B) magnified spectrum showing the peak of MnO_2 at 2θ = 38.6 °. The remaining peaks correspond to the Fe_3O_4 structure.

Table S1. Table presenting X-ray diffraction peaks, their corresponding characteristics (height, full width at half maximum, atomic spacing, relevant intensity,andMiller indices) and the reference material.

Pos. [2θ °]	Height [cts]	FWHM [2θ °]	d-spacing [Å]	Rel. Int. [%]	Crystal lattice values	Matched by
18.2673	389.44	0.1535	4.85868	9.75	111	01-088-0866
30.0833	1255.28	0.2558	2.97185	31.44	220	01-088-0866
35.4372	3992.20	0.3326	2.53418	100.00	311	01-088-0866
37.0519	217.58	0.2558	2.42736	5.45	222	01-088-0866
38.5983	81.40	0.1535	2.33360	2.04	211	00-011-0055
40.5006	309.47	0.3070	2.22828	7.75	-	01-076-0123
43.0936	689.83	0.2047	2.10002	17.28	400	01-088-0866
53.4315	264.65	0.4605	1.71556	6.63	422	01-076-0123; 01-088-0866
56.9752	673.24	0.5628	1.61699	16.86	511	01-088-0866
62.5830	881.93	0.1791	1.48492	22.09	440	00-011-0055; 01-076-0123; 01-088-0866
65.9179	49.60	0.3000	1.41765	1.24	-	01-088-0866
71.0806	73.66	0.4093	1.32683	1.85	620	01-088-0866
74.0204	101.66	0.6240	1.27966	2.55	533	00-011-0055; 01-076-0123; 01-088-0866

Table S2. Reference codes and reference materials that were used to characterize the XRD spectrum

Visible	Ref. Code	Score	Compound Name	Displacement [°2Th.]	Scale Factor	Chemical Formula
*	00-011-0055	40	Ramsdellite	-0.321	0.040	MnO_2
*	01-076-0123	41	Iron Oxide Hydroxide	-0.219	0.087	FeOOH
*	01-088-0866	98	Magnetite (Cr-bearing)	-0.092	0.923	Fe_3O_4

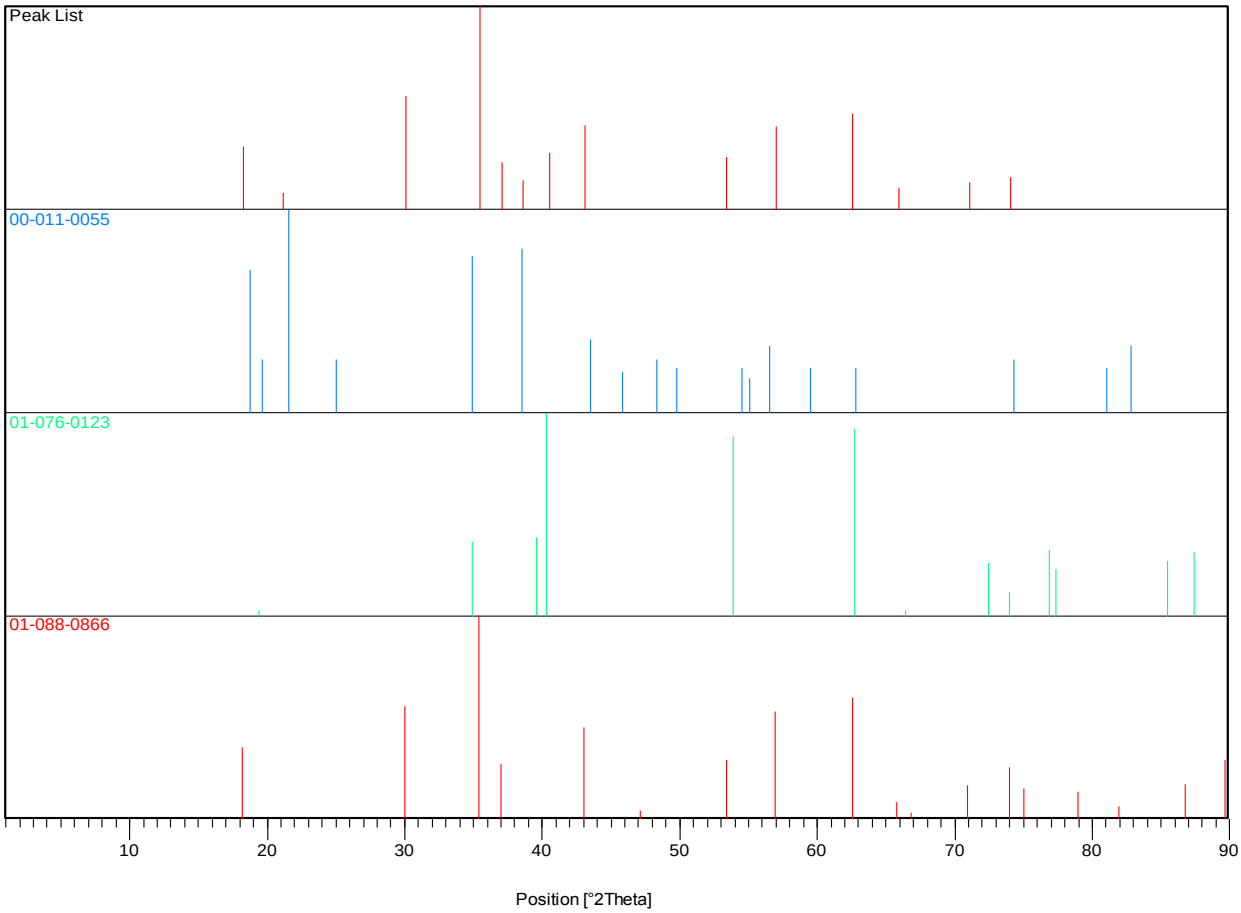

Figure S3. A) X-ray diffraction patterns of the reference materials presented in Table S2.

X-ray photoelectron spectroscopy

Table S3. Elemental analysis of the surface of the NCubes obtained by using X-ray photoelectron spectroscopy

Element	Peak	Position (eV)	FWHM	% Conc.	%At. rel.
C	C-C/C-H	284.6	2.676	12.8	12.8
O	O 1s	529.9	2.309	51.1	58.3
	O 1s	532.2	2.309	7.2	
N	N 1s	399.6	2.086	2.1	2.1
Fe	Fe 2p 3/2 (3+)	711.2	3.807	5.2	19.1
	Fe 2p 1/2 (3+)	724.9	3.275	2.6	
	Fe 2p 3/2 sat (3+)	719.0	5.578	3.3	
	Fe 2p 1/2 (3+)	732.1	6.251	1.7	
	Fe 2p 3/2 (2+)	710.2	2.418	2.4	
	Fe 2p 1/2 (2+)	723.3	2.695	1.2	
	Fe 2p 3/2 sat (2+)	713.9	3.982	1.8	
	Fe 2p 1/2 (2+)	727.4	3.09	0.9	
Mn	Mn 2p 3/2	641.3	3.527	2.3	3.5
	Mn 2p 1/2	653.0	3.648	1.2	
Na	Na 1s	1071.6	2.315	1.6	1.6
Si	Si 2s	152.6	2.997	2.7	2.7

Fe(3+)/Fe(2+) = 2

Table S4. Elemental analysis of the surface of the CM-NCubes obtained by using X-ray photoelectron spectroscopy

Element	Peak	Position (eV)	FWHM	% Conc.	%At. rel.
C	C-C/C-H	284.6	2.625	39.3	47.3
	C-O	287.5	2.362	8.0	
O	O 1s	529.9	2.708	25.8	37.0
	O 1s	531.7	2.708	11.2	
N	N 1s	399.8	2.488	8.6	8.6
Fe	Fe 2p 3/2 (3+)	711.3	3.249	1.9	5.1
	Fe 2p 1/2 (3+)	724.9	3.581	1.0	
	Fe 2p 3/2 sat (3+)	719.1	3.554	0.3	
	Fe 2p 1/2 (3+)	733.6	3.351	0.2	
	Fe 2p 3/2 (2+)	710.1	2.475	0.8	
	Fe 2p 1/2 (2+)	723.0	3.027	0.4	
	Fe 2p 3/2 sat (2+)	713.7	2.932	0.3	
	Fe 2p 1/2 (2+)	727.3	3.512	0.2	
Mn	Mn 2p 3/2	641.6	3.589	1.4	2.1
	Mn 2p 1/2	653.3	3.804	0.7	

Fe(3+)/Fe(2+) = 2

Sodium dodecyl sulfate polyacrylamide gel electrophoresis (SDS-PAGE) and mass spectroscopy

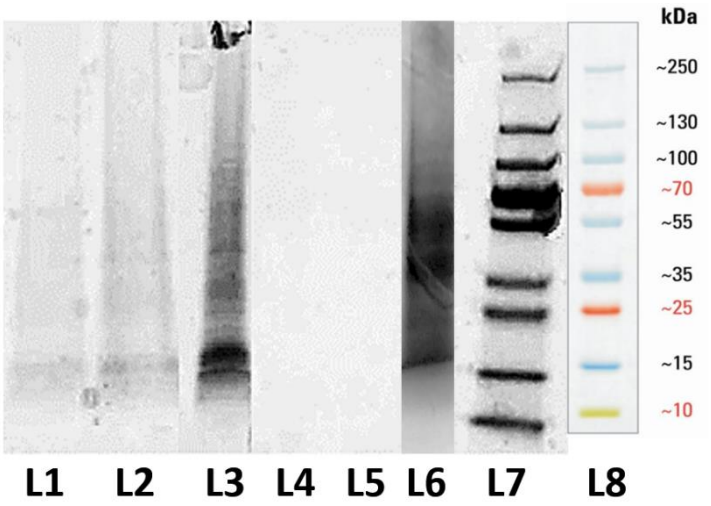

A)

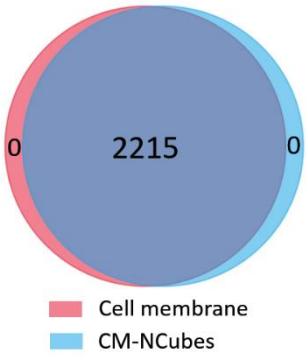

B)

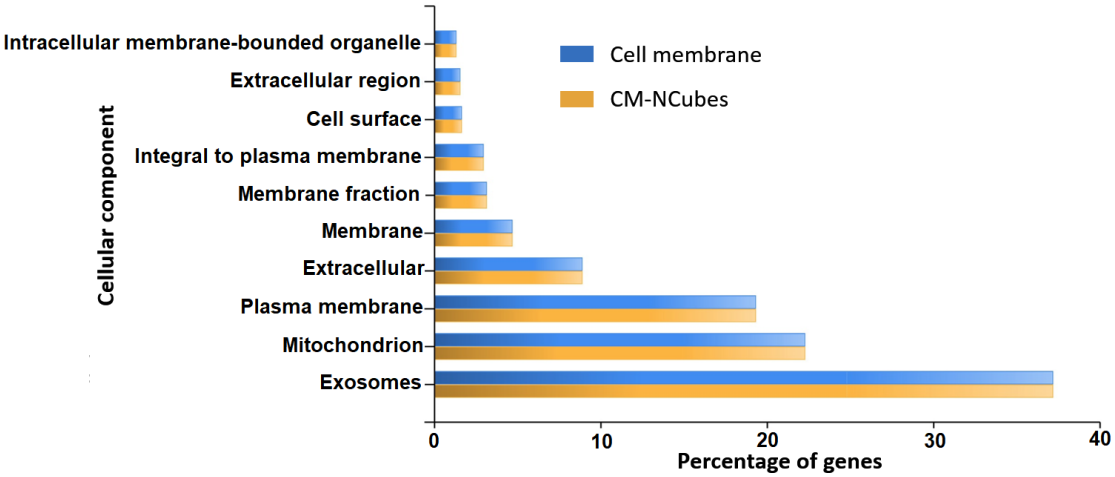

C)

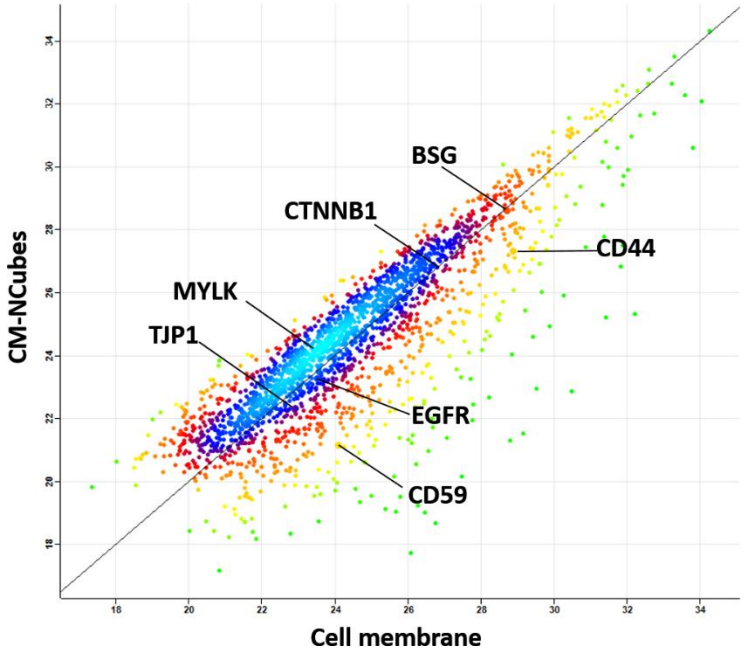

D)

Figure S4. A) SDS-Page of L1) CM-NCubes 3.75µg (125 µg ml^{-1}), L2) CM-NCubes 7.0 µg (250 µg ml^{-1}), L3) CM-NCubes 14 µg (500 µg ml^{-1}), L4) NCubes 7.0 µg (250 µg ml^{-1}), L5) NCubes 14.0 µg (500 µg ml^{-1}), L6) pure cell membrane extracted from 6x10^{6} cells, L7) marker, L8) molecular weight ladder; B) Venn diagram presenting the number of common proteins found on the purified cell membrane and on the surface of CM-NCubes; C) bar chart, derived from mass spectroscopy analysis, presenting the proteins per cell compartment for the extracted cell membrane (blue bars) and for the CM-NCubes (yellow bar) – x axis represents the percentage of the genes associated with the proteins of the membrane presented in the y axis- and D) Volcano plot derived from the mass spectroscopy data demonstrating that the proteins found on the surface of the CM-NCubes are the same as the proteins from the extracted cell membrane.

N_2 adsorption-desorption and BET analysis

Figure S4a shows the adsorption volume of N_2 as a function of the relative pressure of N_2 at 77 K. These data show a continuous uptake up to P/P_0 of 0.8; above this value, a sharp increase in adsorbed volume occurs. These effects are attributed to the presence of two types of pores within NCubes: one related to the presence of intrapores in the lower mesopore range (ca. 2 nm) and one related to the interparticle pore volume (>10 nm in size) (Fig. S4b). This sample shows a BET surface area of 34 m^2 g^{-1}, as derived from the formation of the first N_2 monolayer at relative pressures corresponding to pores around 2 nm.

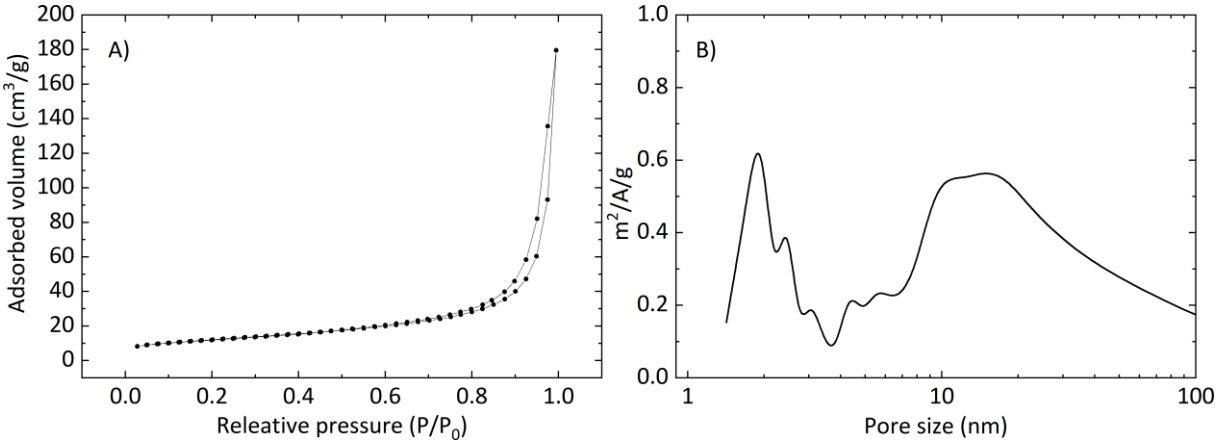

Figure S5. A) Isotherm curves generated during the adsorption and desorption of nitrogen from NCubes, B) Pore size distribution of NCubes

Nitrogen physisorption isotherms were obtained at 77 K on Autosorb 1C (Quantachrome) automatic device. Samples were previously degassed at 423 K for 3 h. The pore size distribution was derived using the Barrett–Joyner–Halenda (BJH) method. [1] The specific surface area was calculated using the Brunauer–Emmett–Teller (BET) method:

$$\frac{1}{v\left[\left(\frac{P_{sat}}{P}\right)-1\right]} = \frac{c-1}{v_m c}\frac{P}{P_{sat}} + \frac{1}{v_m c} \qquad \text{Eq. (1)}$$

where P is the N_2 gas-phase pressure; P_{sat}, N_2 saturation pressure; v, adsorbed gas quantity in volume units; v_m, the monolayer gas quantity.

Stability Studies

NCubes

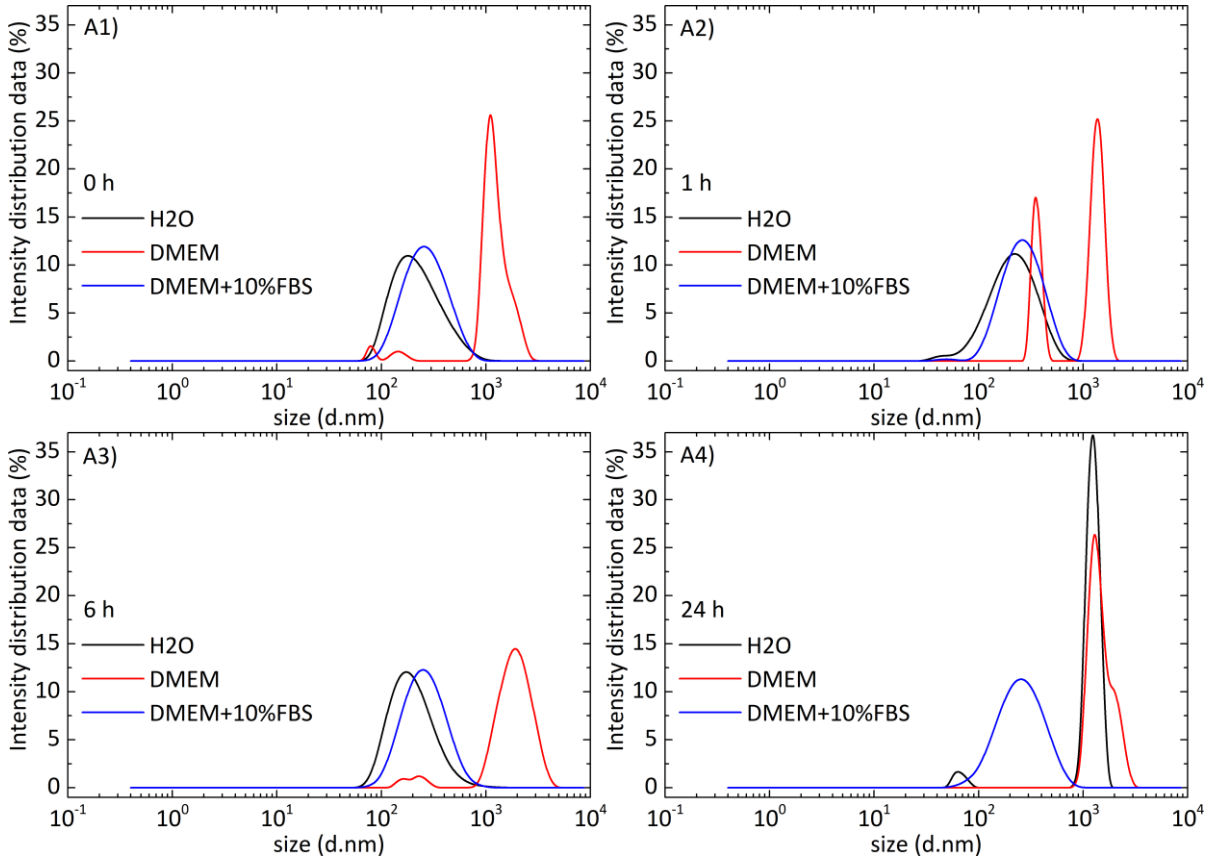

CM-NCubes

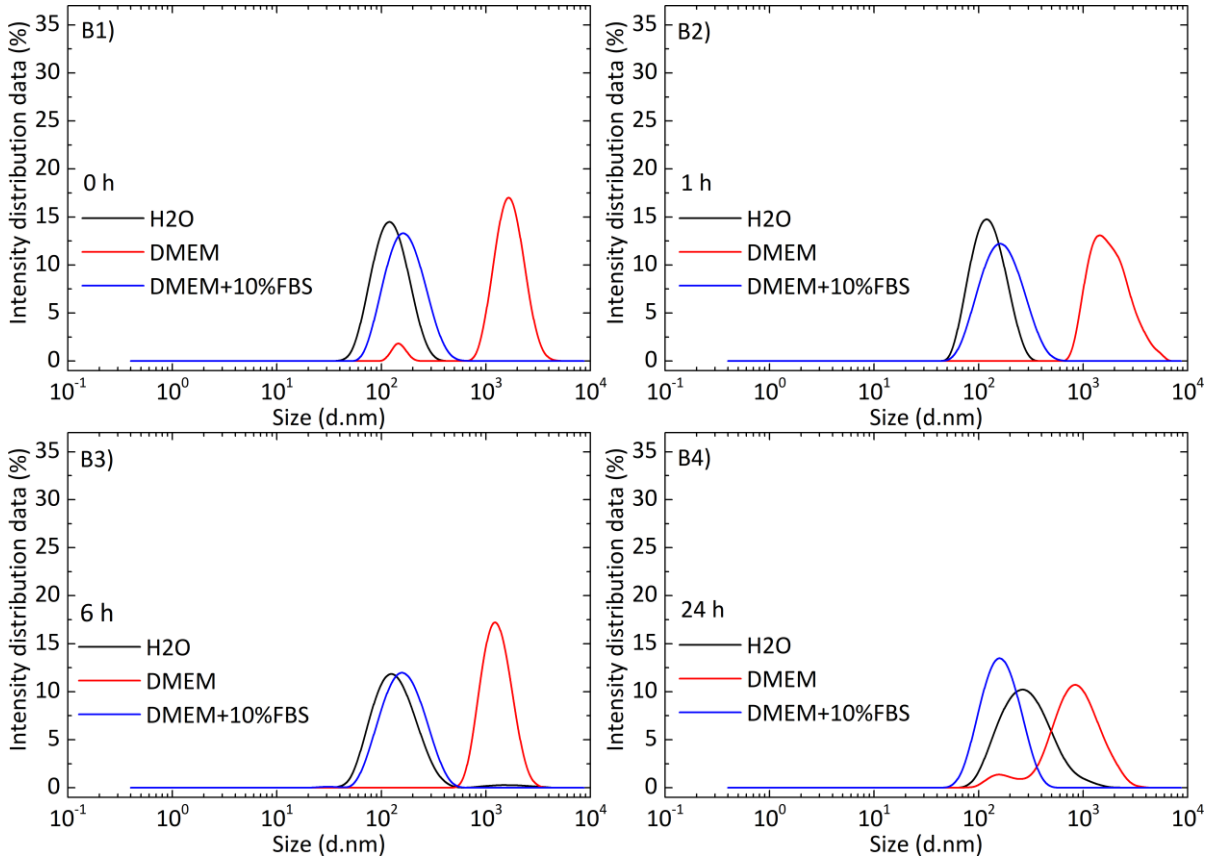

Figure S6. Stability of NCubes (A1-A4) and of CM-NCubes (B1-B4) in different dispersants (H_2O, DMEM and DMEM+10%FBS) and at different time points (0, 1, 6 and 24 h)

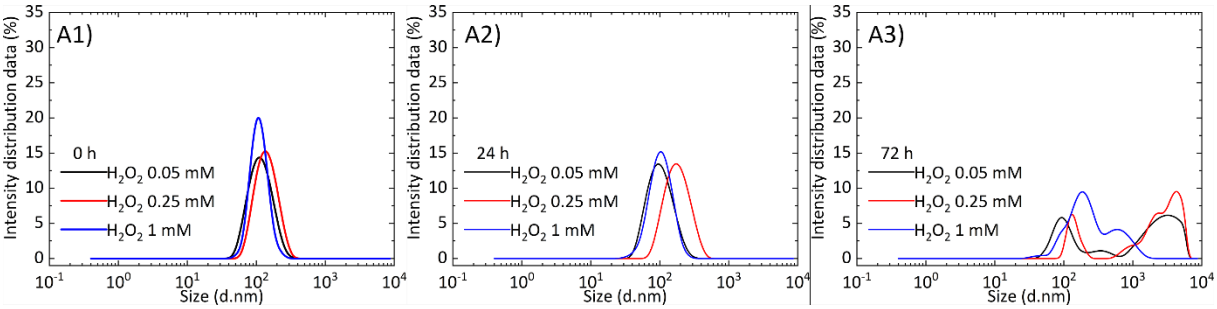

Figure S7. Stability investigation with increasing concentrations of H_2O_2 in aCSF + albumin, simulating oxidative stress.

Nuclear magnetic resonance studies

Table S5. Relaxivity values (r_1 and r_2) of CM-NCubes at various NMR conditions

Frequency [MHz]	T1 [ms]	r1 [$s^{-1}mM^{-1}$]	Err r1 [$s^{-1}mM^{-1}$]	T2 [ms]	r2 [$s^{-1}mM^{-1}$]	Err r2 [$s^{-1}mM^{-1}$]
56.7	999.7	1.76	0.14	14.5	174.60	13.97
21.3	333.0	6.86	0.55	13.7	184.80	14.78
8.5	137.0	17.63	1.41	13.9	182.13	14.57

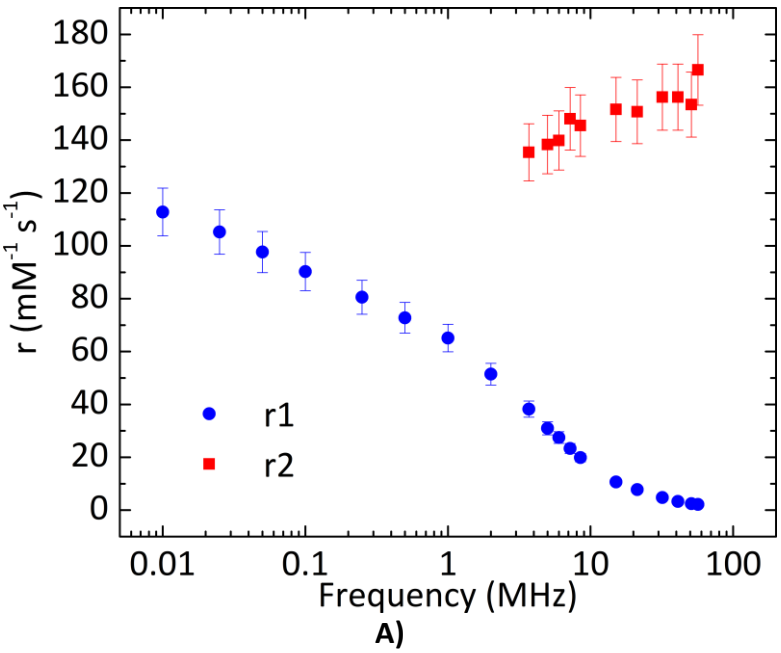

A)

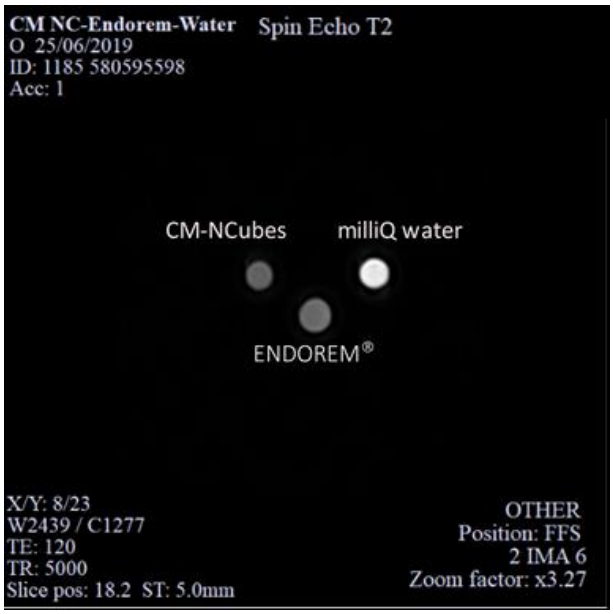

B)

Figure S8. A) Longitudinal r_1 (blue dots) and transverse r_2 (red square) NMR-D profiles collected at room temperature in the frequency range 0.01 < ν < 60 MHz; B) MRI images of vials containing a CM-NCubes dispersion (left, at a concentration of magnetic part equal to 0.08 mM), milliQ water (right) and Endorem® (bottom, at a concentrations of the magnetic part equal to 0.1 mM) obtained by Artoscan (by Esaote SpA) imager at 8.5 MHz by means of high resolution Spin Echo sequence.

Antioxidant capacity

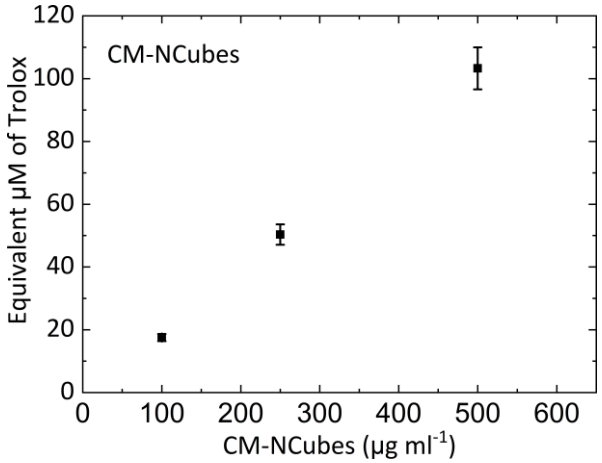

Figure S9. Antioxidant capacity of increasing concentrations of CM-NCubes (100, 250 and 500 µg ml^{-1}), calculated by using Trolox as a standard.

Temperature increase due to ROS scavenging

Video S1. Control sample showing stable fluorescence intensity; U-251 MG cells incubated with 250 µg $ml^{-1}$of CM-NCubes overnight, after the addition of plain DMEM supplemented with 25 mM HEPES

Video S2. Treated sample showing a decrease in fluorescence intensity; U-251 MG cells incubated with 250 µg ml^{-1} of CM-NCubes overnight, after the addition of 100 µM of H_2O_2

Video S3. Negative **c**ontrol sample showing stable fluorescence intensity; U-251 MG cells incubated after the addition of 100 µM of H_2O_2 diluted in complete DMEM supplemented with 25 mM HEPES

Sorafenib release studies

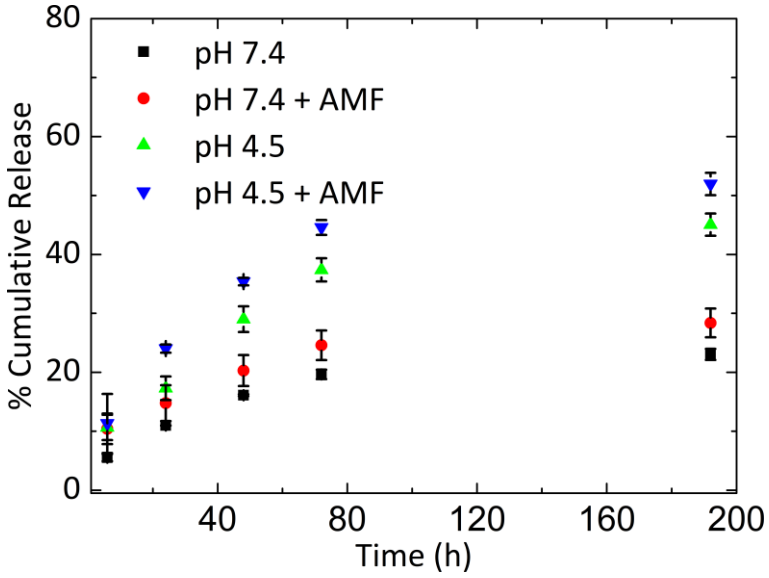

Figure S10. Release profile of the drug sorafenib with and without the use of an AMF and at two different pH values (pH 7.4, pH 4.5, pH7.4+AMF and pH 4.5+AMF). The data are given as the Mean ± SD of three technical replicates.

Table S6. Statistical analysis data of lipid-coated (LP) and cell membrane-coated (CM) nanocubes internalized by C8-D1A, bEnd.3, U-251 MG and SH-SY5Y cell lines after 4 and 24 h. The statistical method used was one-way ANOVA; ns = not significant, *$p < 0.05$, ** $p < 0.01$, *** $p < 0.001$, **** $p < 0.0001$

Bonferroni's multiple comparisons tests	Mean Diff.	95.00% CI of diff.	Significant	Summary
C8-D1A-4 h-LP-NCubes vs. C8-D1A-4 h-CM-NCubes	-3.970	-20.07 to 12.13	No	ns
C8-D1A-4 h-LP-NCubes vs. bEnd.3-4 h-LP-NCubes	-56.47	-72.57 to -40.37	Yes	****
C8-D1A-4 h-LP-NCubes vs. bEnd.3-4 h-CM-NCubes	-45.96	-62.06 to -29.85	Yes	****
C8-D1A-4 h-LP-NCubes vs. U-251 MG-4 h-LP-NCubes	-28.02	-44.12 to -11.92	Yes	**
C8-D1A-4 h-LP-NCubes vs. U-251 MG-4 h-CM-NCubes	-53.61	-69.71 to -37.51	Yes	****
C8-D1A-4 h-LP-NCubes vs. SH-SY5Y-4 h-LP-NCubes	3.775	-12.33 to 19.88	No	ns
C8-D1A-4 h-LP-NCubes vs. SH-SY5Y-4 h-CM-NCubes	-9.080	-25.18 to 7.023	No	ns
C8-D1A-4 h-CM-NCubes vs. bEnd.3-4 h-LP-NCubes	-52.50	-68.60 to -36.40	Yes	****
C8-D1A-4 h-CM-NCubes vs. bEnd.3-4 h-CM-NCubes	-41.99	-58.09 to -25.88	Yes	****
C8-D1A-4 h-CM-NCubes vs. U-251 MG-4 h-LP-NCubes	-24.05	-40.15 to -7.947	Yes	**
C8-D1A-4 h-CM-NCubes vs. U-251 MG-4 h-CM-NCubes	-49.64	-65.74 to -33.54	Yes	****
C8-D1A-4 h-CM-NCubes vs. SH-SY5Y-4 h-LP-NCubes	7.745	-8.358 to 23.85	No	ns
C8-D1A-4 h-CM-NCubes vs. SH-SY5Y-4 h-CM-NCubes	-5.110	-21.21 to 10.99	No	ns
bEnd.3-4 h-LP-NCubes vs. bEnd.3-4 h-CM-NCubes	10.52	-5.588 to 26.62	No	ns
bEnd.3-4 h-LP-NCubes vs. U-251 MG-4 h-LP-NCubes	28.45	12.35 to 44.55	Yes	**
bEnd.3-4 h-LP-NCubes vs. U-251 MG-4 h-CM-NCubes	2.860	-13.24 to 18.96	No	ns
bEnd.3-4 h-LP-NCubes vs. SH-SY5Y-4 h-LP-NCubes	60.25	44.14 to 76.35	Yes	****
bEnd.3-4 h-LP-NCubes vs. SH-SY5Y-4 h-CM-NCubes	47.39	31.29 to 63.49	Yes	****
bEnd.3-4 h-CM-NCubes vs. U-251 MG-4 h-LP-NCubes	17.94	1.832 to 34.04	Yes	*
bEnd.3-4 h-CM-NCubes vs. U-251 MG-4 h-CM-NCubes	-7.655	-23.76 to 8.448	No	ns
bEnd.3-4 h-CM-NCubes vs. SH-SY5Y-4 h-LP-NCubes	49.73	33.63 to 65.83	Yes	****
bEnd.3-4 h-CM-NCubes vs. SH-SY5Y-4 h-CM-NCubes	36.88	20.77 to 52.98	Yes	***
U-251 MG-4 h-LP-NCubes vs. U-251 MG-4 h-CM-NCubes	-25.59	-41.69 to -9.487	Yes	**
U-251 MG-4 h-LP-NCubes vs. SH-SY5Y-4 h-LP-NCubes	31.80	15.69 to 47.90	Yes	***
U-251 MG-4 h-LP-NCubes vs. SH-SY5Y-4 h-CM-NCubes	18.94	2.837 to 35.04	Yes	*
U-251 MG-4 h-CM-NCubes vs. SH-SY5Y-4 h-LP-NCubes	57.39	41.28 to 73.49	Yes	****
U-251 MG-4 h-CM-NCubes vs. SH-SY5Y-4 h-CM-NCubes	44.53	28.43 to 60.63	Yes	****
SH-SY5Y-4 h-LP-NCubes vs. SH-SY5Y-4 h-CM-NCubes	-12.86	-28.96 to 3.248	No	ns

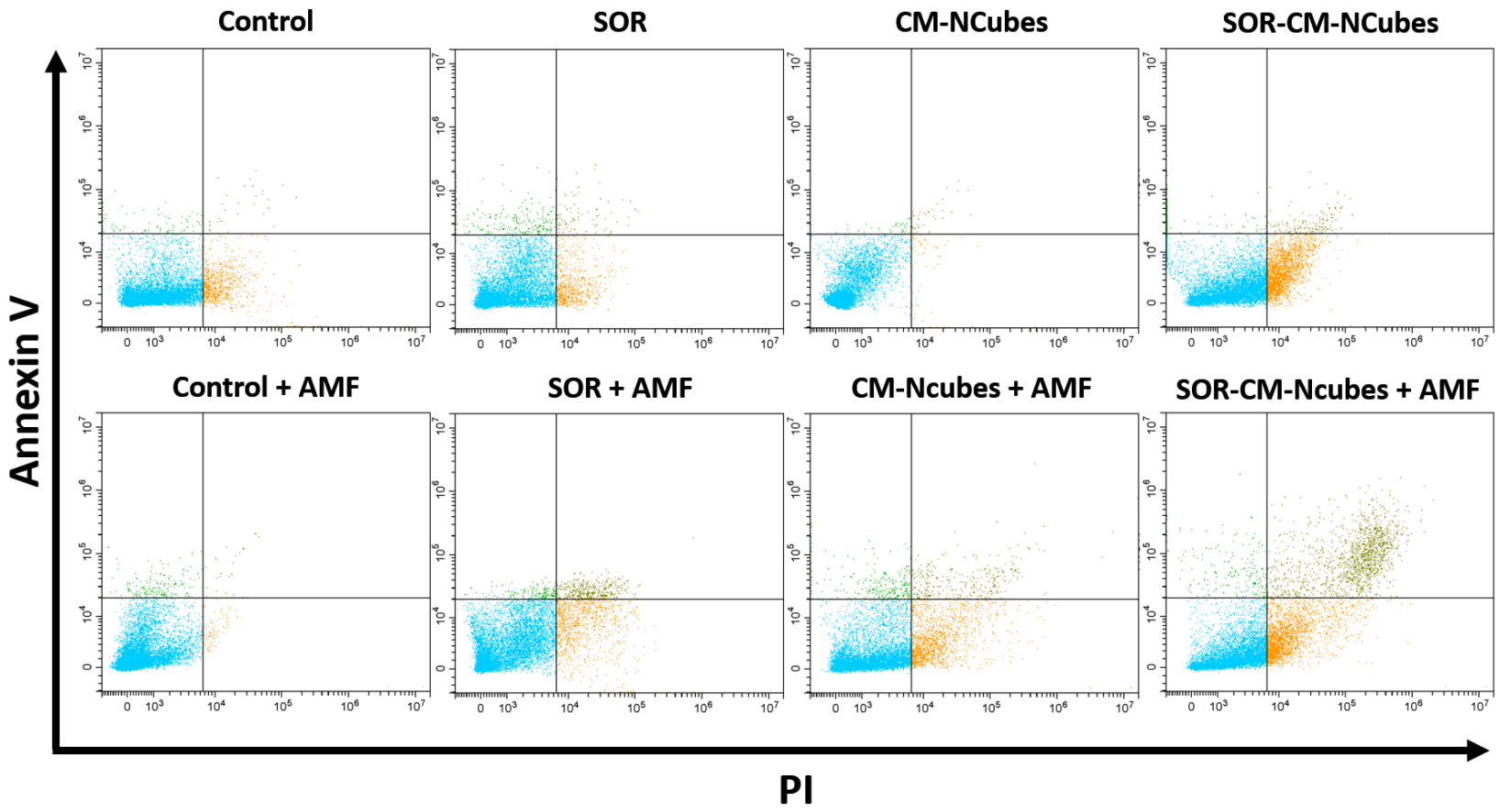

Figure S11. Representative flow cytometry plots depicting viable, early apoptotic, late apoptotic and necrotic cell populations under various treatments

Table S7. Statistical analysis data of caspase 3 activation levels, after treatment with free sorafenib, with cell membrane-coated nanocubes (CM-NCubes), and with cell membrane-coated nanocubes loaded with sorafenib (SOR-CM-NCubes), without and with exposure to an alternating magnetic field (AMF). The statistical method used was one-way ANOVA; ns = not significant, *$p < 0.05$, **$p < 0.01$, ***$p < 0.001$, ****$p < 0.0001$.

Bonferroni's multiple comparisons test	Mean Diff.	95.00% CI of diff.	Significant?	Summary
CTRL vs. SOR	0.4443	-1.436 to 2.325	No	ns
CTRL vs. CM-NCubes	0.001446	-1.879 to 1.882	No	ns
CTRL vs. SOR-CM-NCubes	-0.9745	-2.855 to 0.9063	No	ns
CTRL vs. CTRL+AMF	0.1860	-1.695 to 2.067	No	ns
CTRL vs. SOR+AMF	-0.1658	-2.046 to 1.715	No	ns
CTRL vs. CM-NCubes+AMF	-1.089	-2.970 to 0.7916	No	ns
CTRL vs. SOR-CM-NCubes+AMF	-1.977	-3.858 to -0.09664	Yes	*
SOR vs. CM-NCubes	-0.4429	-2.324 to 1.438	No	ns
SOR vs. SOR-CM-NCubes	-1.419	-3.300 to 0.4619	No	ns
SOR vs. CTRL+AMF	-0.2583	-2.139 to 1.622	No	ns
SOR vs. SOR+AMF	-0.6101	-2.491 to 1.271	No	ns
SOR vs. CM-NCubes+AMF	-1.533	-3.414 to 0.3472	No	ns
SOR vs. SOR-CM-NCubes+AMF	-2.422	-4.302 to -0.5410	Yes	**
CM-NCubes vs. SOR-CM-NCubes	-0.9759	-2.857 to 0.9048	No	ns
CM-NCubes vs. CTRL+AMF	0.1846	-1.696 to 2.065	No	ns
CM-NCubes vs. SOR+AMF	-0.1672	-2.048 to 1.713	No	ns
CM-NCubes vs. CM-NCubes+AMF	-1.091	-2.971 to 0.7901	No	ns
CM-NCubes vs. SOR-CM-NCubes+AMF	-1.979	-3.860 to -0.09809	Yes	*
SOR-CM-NCubes vs. CTRL+AMF	1.160	-0.7202 to 3.041	No	ns
SOR-CM-NCubes vs. SOR+AMF	0.8087	-1.072 to 2.689	No	ns
SOR-CM-NCubes vs. CM-NCubes+AMF	-0.1147	-1.995 to 1.766	No	ns
SOR-CM-NCubes vs. SOR-CM-NCubes+AMF	-1.003	-2.884 to 0.8778	No	ns
CTRL+AMF vs. SOR+AMF	-0.3518	-2.233 to 1.529	No	ns
CTRL+AMF vs. CM-NCubes+AMF	-1.275	-3.156 to 0.6055	No	ns
CTRL+AMF vs. SOR-CM-NCubes+AMF	-2.163	-4.044 to -0.2827	Yes	*
SOR+AMF vs. CM-NCubes+AMF	-0.9234	-2.804 to 0.9573	No	ns
SOR+AMF vs. SOR-CM-NCubes+AMF	-1.812	-3.692 to 0.06914	No	ns

CM-NCubes+AMF vs. SOR-CM-NCubes+AMF	-0.8882	-2.769 to 0.9925	No	ns

Table S8. Statistical analysis data of the caspase 9 activation levels, after treatment with free sorafenib, with cell membrane-coated nanocubes (CM-NCubes), and with cell membrane-coated nanocubes loaded with sorafenib (SOR-CM-NCubes), without and with exposure to an alternating magnetic field (AMF). The statistical method used was one-way ANOVA; ns = not significant, *$p < 0.05$, **$p < 0.01$, ***$p < 0.001$, ****$p < 0.0001$.

Bonferroni's multiple comparisons test	Mean Diff.	95.00% CI of diff.	Significant?	Summary
CTRL vs. SOR	-1.313	-4.245 to 1.620	No	ns
CTRL vs. CM-NCubes	0.1785	-2.754 to 3.111	No	ns
CTRL vs. SOR-CM-NCubes	-2.806	-5.739 to 0.1259	No	ns
CTRL vs. CTRL+AMF	-0.8742	-3.807 to 2.058	No	ns
CTRL vs. SOR+AMF	-2.449	-5.381 to 0.4836	No	ns
CTRL vs. CM-NCubes+AMF	-1.607	-4.539 to 1.325	No	ns
CTRL vs. SOR-CM-NCubes+AMF	-6.539	-9.472 to -3.607	Yes	****
SOR vs. CM-NCubes	1.491	-1.441 to 4.423	No	ns
SOR vs. SOR-CM-NCubes	-1.494	-4.426 to 1.438	No	ns
SOR vs. CTRL+AMF	0.4383	-2.494 to 3.371	No	ns
SOR vs. SOR+AMF	-1.136	-4.069 to 1.796	No	ns
SOR vs. CM-NCubes+AMF	-0.2944	-3.227 to 2.638	No	ns
SOR vs. SOR-CM-NCubes+AMF	-5.227	-8.159 to -2.294	Yes	***
CM-NCubes vs. SOR-CM-NCubes	-2.985	-5.917 to -0.05254	Yes	*
CM-NCubes vs. CTRL+AMF	-1.053	-3.985 to 1.880	No	ns
CM-NCubes vs. SOR+AMF	-2.627	-5.560 to 0.3051	No	ns
CM-NCubes vs. CM-NCubes+AMF	-1.785	-4.718 to 1.147	No	ns
CM-NCubes vs. SOR-CM-NCubes+AMF	-6.718	-9.650 to -3.785	Yes	****
SOR-CM-NCubes vs. CTRL+AMF	1.932	-1.000 to 4.865	No	ns
SOR-CM-NCubes vs. SOR+AMF	0.3577	-2.575 to 3.290	No	ns
SOR-CM-NCubes vs. CM-NCubes+AMF	1.200	-1.733 to 4.132	No	ns
SOR-CM-NCubes vs. SOR-CM-NCubes+AMF	-3.733	-6.665 to -0.8003	Yes	**
CTRL+AMF vs. SOR+AMF	-1.575	-4.507 to 1.358	No	ns
CTRL+AMF vs. CM-NCubes+AMF	-0.7327	-3.665 to 2.200	No	ns
CTRL+AMF vs. SOR-CM-NCubes+AMF	-5.665	-8.597 to -2.733	Yes	****

SOR+AMF vs. CM-NCubes+AMF	0.8419	-2.091 to 3.774	No	ns
SOR+AMF vs. SOR-CM-NCubes+AMF	-4.090	-7.023 to -1.158	Yes	**
CM-NCubes+AMF vs. SOR-CM-NCubes+AMF	-4.932	-7.865 to -2.000	Yes	***

Table S9. Statistical analysis data of ROS generation, after treatment with free sorafenib, with cell membrane-coated nanocubes (CM-NCubes), and with cell membrane-coated nanocubes loaded with sorafenib (SOR-CM-NCubes), without and with their exposure to an alternating magnetic field (AMF). The statistical method used was one-way ANOVA; ns = not significant, *$p < 0.05$, **$p < 0.01$, ***$p < 0.001$, ****$p < 0.0001$.

Bonferroni's multiple comparisons test	Mean Diff.	95.00% CI of diff.	Significant?	Summary
CTRL vs. SOR	0.1344	-2.182 to 2.450	No	ns
CTRL vs. CM-NCubes	-1.066	-3.381 to 1.250	No	ns
CTRL vs. SOR-CM-NCubes	-2.258	-4.574 to 0.05757	No	ns
CTRL vs. CTRL+AMF	0.1126	-2.203 to 2.429	No	ns
CTRL vs. SOR+AMF	-0.8054	-3.121 to 1.511	No	ns
CTRL vs. CM-NCubes+AMF	-4.544	-6.860 to -2.228	Yes	****
CTRL vs. SOR-CM-NCubes+AMF	-3.601	-5.917 to -1.285	Yes	***
SOR vs. CM-NCubes	-1.200	-3.516 to 1.116	No	ns
SOR vs. SOR-CM-NCubes	-2.393	-4.709 to -0.07684	Yes	*
SOR vs. CTRL+AMF	-0.02184	-2.338 to 2.294	No	ns
SOR vs. SOR+AMF	-0.9399	-3.256 to 1.376	No	ns
SOR vs. CM-NCubes+AMF	-4.678	-6.994 to -2.362	Yes	****
SOR vs. SOR-CM-NCubes+AMF	-3.735	-6.051 to -1.419	Yes	***
CM-NCubes vs. SOR-CM-NCubes	-1.193	-3.509 to 1.123	No	ns
CM-NCubes vs. CTRL+AMF	1.178	-1.138 to 3.494	No	ns
CM-NCubes vs. SOR+AMF	0.2601	-2.056 to 2.576	No	ns
CM-NCubes vs. CM-NCubes+AMF	-3.478	-5.794 to -1.162	Yes	**
CM-NCubes vs. SOR-CM-NCubes+AMF	-2.535	-4.851 to -0.2193	Yes	*
SOR-CM-NCubes vs. CTRL+AMF	2.371	0.05500 to 4.687	Yes	*
SOR-CM-NCubes vs. SOR+AMF	1.453	-0.8630 to 3.769	No	ns
SOR-CM-NCubes vs. CM-NCubes+AMF	-2.285	-4.601 to 0.03069	No	ns
SOR-CM-NCubes vs. SOR-CM-NCubes+AMF	-1.342	-3.658 to 0.9736	No	ns

CTRL+AMF vs. SOR+AMF	-0.9180	-3.234 to 1.398	No	ns
CTRL+AMF vs. CM-NCubes+AMF	-4.656	-6.972 to -2.340	Yes	****
CTRL+AMF vs. SOR-CM-NCubes+AMF	-3.713	-6.029 to -1.397	Yes	***
SOR+AMF vs. CM-NCubes+AMF	-3.738	-6.054 to -1.422	Yes	***
SOR+AMF vs. SOR-CM-NCubes+AMF	-2.795	-5.111 to -0.4794	Yes	**
CM-NCubes+AMF vs. SOR-CM-NCubes+AMF	0.9429	-1.373 to 3.259	No	ns

Table S10. Statistical analysis data of RNS generation, after treatment with free sorafenib, with cell membrane-coated nanocubes (CM-NCubes), and with cell membrane-coated nanocubes loaded with sorafenib (SOR-CM-NCubes), without and with their exposure to an alternating magnetic field (AMF). The statistical method used was one-way ANOVA; ns = not significant, *$p < 0.05$, **$p < 0.01$, ***$p < 0.001$, ****$p < 0.0001$.

Bonferroni's multiple comparisons test	Mean Diff.	95.00% CI of diff.	Significant?	Summary
CTRL vs. SOR	-0.9876	-3.067 to 1.091	No	ns
CTRL vs. CM-NCubes	-0.9850	-3.064 to 1.094	No	ns
CTRL vs. SOR-CM-NCubes	0.1495	-1.929 to 2.228	No	ns
CTRL vs. CTRL+AMF	0.1795	-1.900 to 2.258	No	ns
CTRL vs. SOR+AMF	-0.08655	-2.166 to 1.992	No	ns
CTRL vs. CM-NCubes+AMF	-0.3061	-2.385 to 1.773	No	ns
CTRL vs. SOR-CM-NCubes+AMF	-0.5804	-2.659 to 1.499	No	ns
SOR vs. CM-NCubes	0.002623	-2.076 to 2.082	No	ns
SOR vs. SOR-CM-NCubes	1.137	-0.9419 to 3.216	No	ns
SOR vs. CTRL+AMF	1.167	-0.9119 to 3.246	No	ns
SOR vs. SOR+AMF	0.9011	-1.178 to 2.980	No	ns
SOR vs. CM-NCubes+AMF	0.6815	-1.397 to 2.761	No	ns
SOR vs. SOR-CM-NCubes+AMF	0.4073	-1.672 to 2.486	No	ns
CM-NCubes vs. SOR-CM-NCubes	1.135	-0.9445 to 3.213	No	ns
CM-NCubes vs. CTRL+AMF	1.164	-0.9145 to 3.243	No	ns
CM-NCubes vs. SOR+AMF	0.8985	-1.181 to 2.977	No	ns
CM-NCubes vs. CM-NCubes+AMF	0.6789	-1.400 to 2.758	No	ns
CM-NCubes vs. SOR-CM-NCubes+AMF	0.4046	-1.674 to 2.484	No	ns
SOR-CM-NCubes vs. CTRL+AMF	0.02997	-2.049 to 2.109	No	ns
SOR-CM-NCubes vs. SOR+AMF	-0.2360	-2.315 to 1.843	No	ns

SOR-CM-NCubes vs. CM-NCubes+AMF	-0.4556	-2.535 to 1.623	No	ns
SOR-CM-NCubes vs. SOR-CM-NCubes+AMF	-0.7299	-2.809 to 1.349	No	ns
CTRL+AMF vs. SOR+AMF	-0.2660	-2.345 to 1.813	No	ns
CTRL+AMF vs. CM-NCubes+AMF	-0.4856	-2.565 to 1.593	No	ns
CTRL+AMF vs. SOR-CM-NCubes+AMF	-0.7598	-2.839 to 1.319	No	ns
SOR+AMF vs. CM-NCubes+AMF	-0.2196	-2.299 to 1.859	No	ns
SOR+AMF vs. SOR-CM-NCubes+AMF	-0.4938	-2.573 to 1.585	No	ns
CM-NCubes+AMF vs. SOR-CM-NCubes+AMF	-0.2743	-2.353 to 1.805	No	ns

Formation of the U-251 MG tumor spheroids and particle internalization

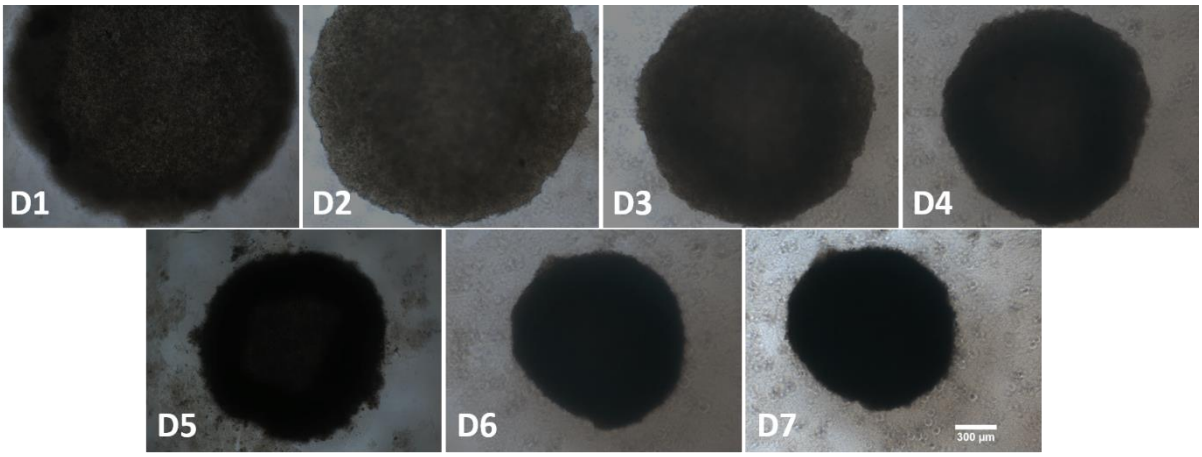

Figure S12. Optical microscopy images during the formation of the U-251 MG spheroids for 7 days. The number of seeded cells is $100 \cdot 10^3$ /well. Scale Bar: 300 µm

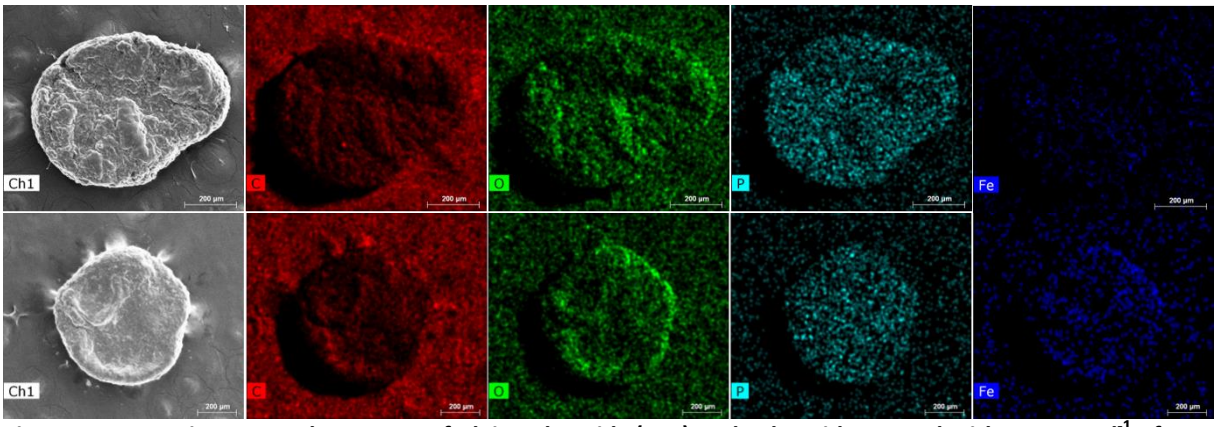

Figure S13. SEM images and EDS map of plain spheroids (top) and spheroids treated with 100 µg ml^{-1} of CM-NCubes for 24 h (bottom). EDS mapping shows an increased percentage of Fe in the CM-NCubes-treated spheroids. Scale bar: 200 µm.

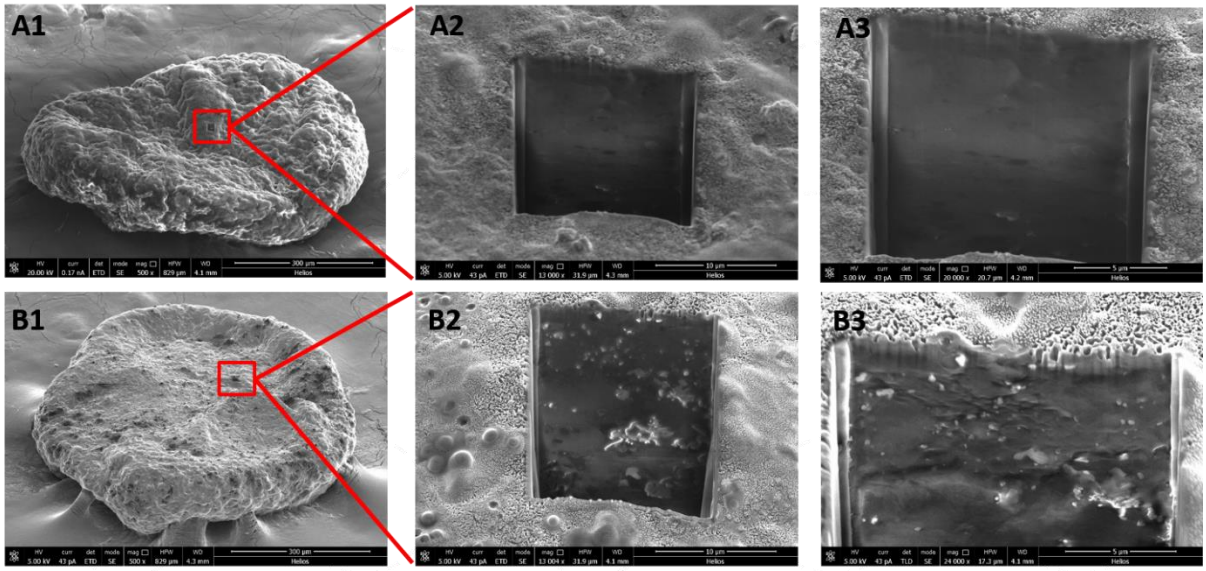

Figure S14. Cross-section (CS) SEM images of plain spheroids (top) and spheroids treated with 100 µg ml^{-1} of CM-NCubes (bottom) for 24 h, where the internalization of the CM-NCubes can be observed. Cross-section depth: 5 µm

Parameters of the numerical model used for magnetic targeting

We exploited the magnetic targeting model detailed in Grillone *et al.*[2]; the involved parameters are listed in **Table S 12** for completeness. A few remarks are hereafter reported:

- channel geometry, fluid properties, as well as magnet geometry and magnetization were taken from Grillone *et al.*[2] (in particular, we defined the flow rate in order to induce a shear stress value typical of capillaries, namely 1 Pa);
- we derived the magneto-responsive volume fraction (denoted by β_m in Grillone *et al.*[2] from the measured mass fractions, namely 10.5 for the Fe/Mn (as calculated by ICP) and 88/12 for the inorganic phase / cell membrane coating (as calculated by TGA) (we assumed the following densities: 7870 kg m^{-3} for Fe, 7430 kg m^{-3} for Mn and 1070 kg m^{-3} for cell membrane;[3]
- we derived the saturation magnetization of the magneto responsive phase from the measured value for CM-NCubes (**Fig. 3A** in the main text);

Table S12. Parameters of the numerical model used for magnetic targeting

Parameter [unit]	Value
Channel height [mm]	0.5
Channel width [mm]	5
Distance between permanent magnet and fluid channel [mm]	0.86
Permanent magnet diameter [mm]	13
Permanent magnet height [mm]	10
Fluid viscosity [Pa s]	1e-3
Flow rate [ml min^{-1}]	12
Permanent magnet magnetization [A m^{-1}]	1.05e6
CM-NCubes radius (coating included) [nm]	10
CM-NCubes magneto-responsive volume fraction [-]	0.50
Saturation magnetization of the magneto-responsive phase [A m^{-1}]	4.47e5

As regards the numerics, we discretized the permanent magnet by means of an equivalent currents model using 1000 current strips, and we used 40 modes to reconstruct the fluid flow (Grillone *et al.*[2] for details). Moreover, we virtually seeded 1248000 CM-NCubes upstream enough from the magnet (half-cross section, by symmetry), and we integrated their trajectory using the Matlab numerical environment, up to impinging on either the channel floor (capture condition) or the outflow cross-section (escape condition). Captured

carriers were then binned (bin size 100 µm) in order to render the capture density through a contour plot (**Fig. 7C** in the main text).

Bibliography

1. S. Brunauer, P. H. Emmett and E. Teller, *Journal of the American Chemical Society*, 1938, **60**, 309-319.
2. A. Grillone, M. Battaglini, S. Moscato, L. Mattii, C. de Julian Fernandez, A. Scarpellini, M. Giorgi, E. Sinibaldi and G. Ciofani, *Nanomedicine (Lond)*, 2019, **14**, 727-752.
3. T. E. Thompson, Lipids, https://www.britannica.com/science/lipid/Classification-and-formation, (accessed April 01, 2019).